Helical Structures

DOI: 10.1002/anie.201309172

Inversion of Supramolecular Helicity in Oligo-*p*-phenylene-Based Supramolecular Polymers: Influence of Molecular Atropisomerism**

Fátima Aparicio, Belén Nieto-Ortega, Francisco Nájera, Francisco J. Ramírez, Juan T. López Navarrete, Juan Casado,* and Luis Sánchez**

Abstract: *The helical organization of oligo-p-phenylene-based organogelators has been investigated by atomic force microscopy, circular and vibrational circular dichroism, and Raman techniques. Whilst OPPs with more than two phenyl rings in the core self-assemble into left-handed helices, that with a biphenyl core shows an inversion of the supramolecular helicity depending on the formation conditions through the atropisomerism of the biphenyl central unit. The results presented herein outline a new example of kinetically controlled modulation of supramolecular helicity.*

Chirality has been the inspiration for many scientists investigating the processes that yield asymmetric products from originally achiral racemates.[1] Asymmetric chemical synthesis and catalysis,[2] liquid crystals,[3] and conductive materials[4] are examples of the application of chiral structures to different research areas. The term chirality describes the structural property of an object that is non-superimposable on its mirror image and can be achieved by the presence in a molecule of: a) stereogenic centers; b) chiral planes; c) chiral axes, or d) helical chirality. The last is often achieved by the supramolecular polymerization of self-assembling molecules decorated with peripheral side chains containing stereogenic centers that act as the sole inductor element of helical chirality.[5] Besides stereogenic seeds, the influence of other alternative sources of chirality for the generation of, or the interconversion between, left-handed (*M*-type) and right-handed (*P*-type) supramolecular helices remains unprecedented. The control of the helicity in supramolecular ensembles has important mechanistic implications in supramolecular chemistry and is intimately connected with the topic of chirality transmission, which is of high significance in life sciences.

Herein, we report on the influence of the molecular atropisomerism of oligo-*p*-phenylene-based (OPP) organogelators (**1**–**4**; Figure 1) on the helical chirality resulting from their supramolecular polymerization.[6] This helical chirality in **2**–**4** was investigated on surfaces, in solution, and in a gel state by utilizing circular dichroism (CD), vibrational circular dichroism (VCD), and Raman optical activity (ROA) combined with quantum model studies.

Compounds **3** and **4** form robust and stable chiral helical aggregates, while **2** exhibits an exchangeable helicity depending on the reaction time, concentration, and temperature and reveals a new example of kinetic-versus-thermodynamic

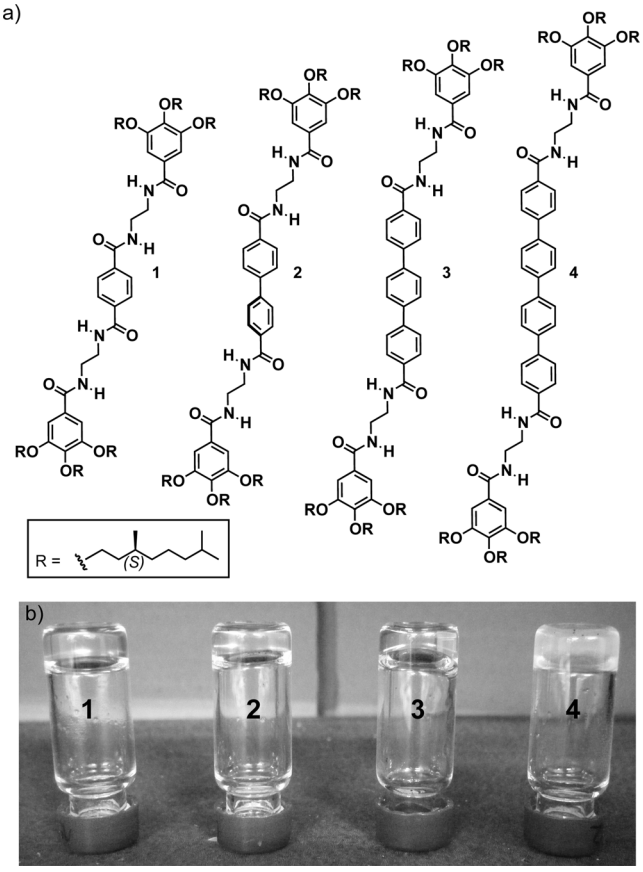

Figure 1. a) Chemical structures of the self-assembling OPP-based organogelators **1**–**4**. b) Photograph of the organogels formed from compounds **1**–**4** in toluene.

[*] F. Aparicio, L. Sánchez
Departamento de Química Orgánica
Facultad de Ciencias Químicas
Ciudad Universitaria s/n, 28040 Madrid (Spain)
E-mail: lusamar@quim.ucm.es
B. Nieto-Ortega, F. J. Ramírez, J. T. López Navarrete, J. Casado
Departamento de Química Física, Facultad de Ciencias
Universidad de Málaga
Campus de Teatinos s/n, 29071 Málaga (Spain)
E-mail: teodomiro@uma.es
casado@uma.es
F. Nájera
Departamento de Química Orgánica, Facultad de Ciencias
Universidad de Málaga
Campus de Teatinos s/n, 29071 Málaga (Spain)

[**] Financial support from the MINECO of Spain (CTQ2011-22581 and CTQ2012-33733) is acknowledged. F.A and B.N.O. are indebted to MEC for their FPU studentship.

Supporting information for this article is available on the WWW under http://dx.doi.org/10.1002/anie.201309172.

competitive modulation of supramolecular helicity.[7] At low temperature, low concentration, and short polymerization times (kinetic control) compound **2** self-assembles into right-handed metastable supramolecular helices, as dictated by the axial chirality of the biphenyl core. In contrast, at higher temperature, higher concentration, and long reaction times (thermodynamic control), the axial chirality in **2** is cancelled out and only the external *S* stereocenters impose a left-handed durable supramolecular helix. In contrast, **3** and **4** self-assemble into left-handed aggregates, with no inversion of their helicity. These findings imply the lack of influence of the oligophenyl atropisomerism in the helical organization of **3** and **4** into their supramolecular aggregates, which is exclusively dictated by the external stereocenters, such as of **2** under thermodynamic conditions. The studies presented here contribute to the understanding of the chemical and topological control in the generation of helical supramolecular structures and the impact of the synergy between different chiral elements.

The preparation of the OPP derivatives **2**–**4** starts with the synthesis of the previously reported *N*-(2-aminoethyl)-3,4,5-tri-((*S*)-3′,7′-dimethyloctyl)oxybenzamide (**5** in Scheme S1 in the Supporting Information),[8] which is coupled with biphenyl-4,4′-dicarboxylic acid to yield **2** or with 4-iodobenzoic acid to give the corresponding iodobisamide. A double Suzuki C–C cross-coupling reaction with benzenediboronic acid bis(pinacol) ester or with 4,4′-biphenyldiboronic acid bis(pinacol) ester in the presence of a palladium catalyst[9] affords compounds **3** and **4**, respectively (see Scheme S1 in the Supporting Information). All the newly reported compounds have been fully characterized by NMR and FTIR spectroscopy as well as by high-resolution mass spectrometry (see the Supporting Information).

The ability of compounds **2**–**4** to self-assemble was first tested by the formation of organogels in apolar solvents such as methylcyclohexane (MCH) and toluene. OPPs **2**–**4**, as reported for **1**,[6] form transparent organogels in toluene (Figure 1b). The formation of organogels is indicative of the generation of columnar supramolecular structures that further aggregate to form bundles of fibers that support the solvent upon inversion of the vial.[10] AFM images of diluted samples of the gel on highly oriented pyrolytic graphite (HOPG) show enantiomerically enriched, helical supramolecular structures (Figure 2, see also Figures S1–S3 in the Supporting Information). The three organogels are organized into ropelike, broad fibers with height profiles of around 3–5 nm. These ropelike fibers exhibit a left-handed (*M*-type) helicity. However, a closer inspection of the AFM images of organogelator **2** shows the presence of chainlike structures, in which the links are clearly visible but the helicity cannot be assigned (Figure 2b and see Figure S1a–c in the Supporting Information).

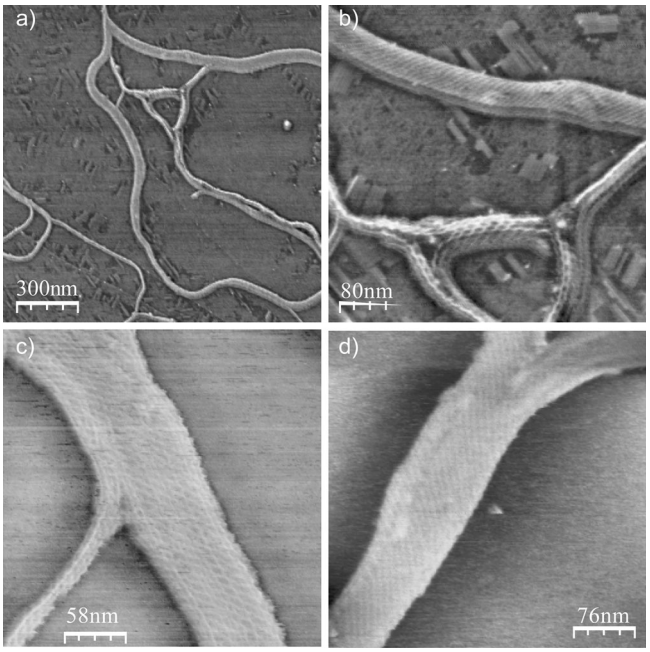

Figure 2. AFM phase images of the diluted gels of **2** (a and b), **3** (c), and **4** (d) on HOPG (1×10^{-5} M, toluene, 298 K).

The helicity of the aggregates formed by OPPs **2**–**4** in solution was first investigated by CD spectroscopy at room temperature (Figure 3a). The CD spectra of compounds **2**–**4** as well as the previously reported **1**[6] exhibit a positive dichroic signal at around 220 nm, which was assigned to an excitation within the peripheral trialkoxybenzamide units. The increasing number of conjugated phenyl groups in **3** and **4** results in a more intense, red-shifted and (+/−) bisignated Cotton UV/Vis band (see Figure S4a in the Supporting Information), which is diagnostic of the presence of *M*-type helical structures in solution (Figure 3a). These experimental

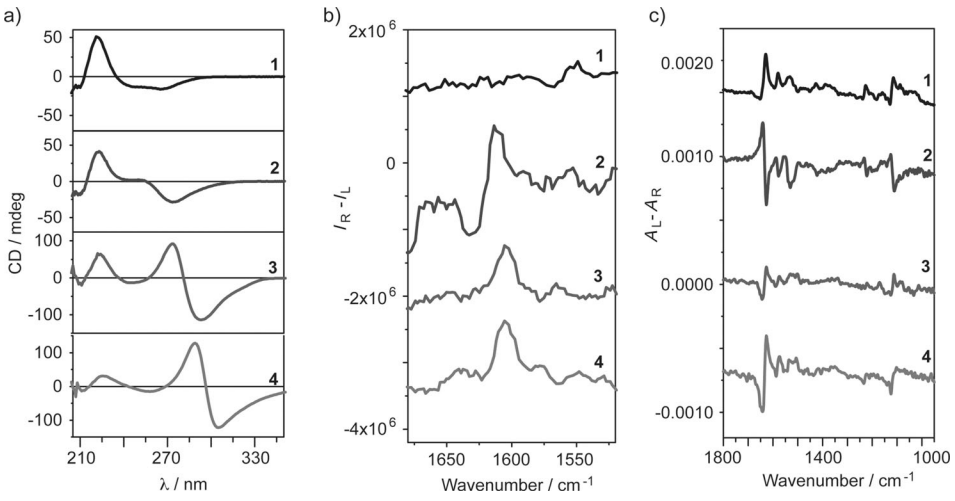

Figure 3. a) Electronic CD spectra (MCH, 1×10^{-5} M, 25 °C); b) ROA spectra (MCH, 3×10^{-3} M, 25 °C); and c) VCD spectra (MCH, 3×10^{-3} M, −25 °C) of compounds **1**–**4**.

data are in good correlation with the helical structures visualized in the AFM images. However, compound **2** shows no clear bisignated CD response, and has a weaker negative band, which suggests the same *M*-type helical organization as in its larger congeners **3** and **4** (Figure 3a). Variable-temperature CD (VT-CD) measurements show nonsigmoidal shapes for the cooling curves of **2**, **3**, and **4**,[12] thus demonstrating the cooperative character of their supramolecular polymerization by self-assembling into *M*-type supramolecular polymers (see Figure S5 in the Supporting Information).[5,13] The presence of more-planar backbones in **3** and **4** induces a more-efficient π-π stacking that stabilizes the helical aggregates, as is suggested by the higher critical temperature at which the nucleation regime changes into an elongation one (see Figure S5 in the Supporting Information).[5]

Raman and ROA spectroscopic studies (298 K, 3×10^{-3} M) were also used to investigate the chiral features of **1–4** (Figure 3b and see Figure S4c in the Supporting Information). The Raman spectra of compounds **2–4** feature a clear Raman band around 1610 cm^{-1} that slightly shifts to lower wavenumbers on going from **2** to **4** (see Figure S4c in the Supporting Information) as a result of the more-efficient conjugation in the cores with more phenyl rings. This conjugation restricts the conformational flexibility of the oligophenyl chains and facilitates intermolecular π-π stacking. This Raman (and ROA) band is not detected in compound **1** because of the absence of conjugation. The spectra of compounds **3** and **4** show strong ROA positive bands at about 1600 cm^{-1}. Again, the ROA spectrum of **2** does not follow the trend observed for **3** and **4**, but shows a negative and a positive signal at 1627 and 1611 cm^{-1}, respectively, thus highlighting its distinctive behavior compared its two larger congeners (Figure 3b).

FTIR and VCD measurements provide valuable information about the molecular-level helicity of the supramolecular aggregates.[13] The vibrational measurements for **1–4** needed to be carried out at a higher concentration (3×10^{-3} M, MCH) and lower temperature (248 K) than those routinely used for the preparation of the corresponding gels. A strong and extensive C=O···H–N hydrogen-bonding network, which significantly stabilizes the supramolecular polymers of **1–4**, is inferred from the vibrational amide I stretching band that appears at around 1631 cm^{-1} (see Figure S4b in the Supporting Information).[5d,e] Whereas this amide I VCD band in **1**, **3**, and **4** has the same (+/−) pattern, that of **2** is the opposite, namely it has a (−/+) signal. This VCD pattern implies the inversion of the chirality from **2** to **1**/**3**/**4** at this concentration and temperature (Figure 3c).

Assuming that the four samples have the same *S*-type of stereocenter, the dissimilar VCD behavior found for compounds **2** and **3**/**4** suggest that their supramolecular polymerization could result in the formation of distinct aggregates of opposite handedness, which was recently reported for the supramolecular polymerization of an oligo(*p*-phenylenevinylene)triazine (*S*-OPV) by either kinetic or thermodynamic pathways.[14] Since the kinetic-versus-thermodynamic competition strongly depends on the experimental conditions, we have investigated the supramolecular polymerization of compounds **2–4** by VCD at different concentrations, temperatures, and times (these are the three parameters that can condition the switch of a kinetic product to the corresponding thermodynamic one). The VCD spectrum of compound **2**, with a (+/−) amide I pattern at 3×10^{-3} M and −25 °C, exhibits the same (+/−) VCD pattern at the same concentration and at 0 °C, while the VCD signal completely vanishes at 25 °C (Table 1 and see Figure S6 in the Supporting Information). Increasing the concentration of **2** to 1.2×10^{-2} M results in an inverted (−/+) pattern for the amide I band at −25 and 0 °C, which persists at 25 °C (Table 1 and see Figure S7 in the Supporting Information). This pattern for **2** at 1.2×10^{-2} M is the same as those of **3** and **4** at all temperatures and concentrations (see Figure S7 in the Supporting Information). These data already indicate that **2** can form different enantiomerically enriched helical supramolecular structures depending on the concentration of the sample, and under these conditions these helices are stable over time.

Table 1: Sign of the VCD amide I band of **2–4** at different concentrations, temperatures, and times in MCH.

Concentration	*T*	**2**	**3**	**4**
	+25 °C	no signal	−/+	−/+
3×10^{-3} M	0 °C	+/−	−/+	−/+
	−25 °C	+/−	−/+	−/+
	+25 °C	+/− (t_0 = 0 h) −/+ (t_f = 24 h)	−/+	−/+
8×10^{-3} M	0 °C	+/− (t_0 = 0 h) [a]	−/+	−/+
	−25 °C	+/− (t_0 = 0 h) [a]	−/+	−/+
	+25 °C	−/+	−/+	−/+
1.2×10^{-2} M	0 °C	−/+	−/+	−/+
	−25 °C	−/+	−/+	−/+

[a] No changes within the 24 h timescale. Possibly longer times are required.

To corroborate the presence of the kinetic-versus-thermodynamic competition in the self-assembly of **2**, VCD experiments were conducted at an intermediate concentration of 8×10^{-3} M as a function of time (Figure 4). At +25 °C and 8×10^{-3} M, compound **2** shows the same (+/−) pattern as that observed for the more dilute sample. Interestingly, keeping this gel at this temperature for 24 h results in the inversion of the amide I band to a (−/+) pattern, a time period that unambiguously demonstrates that the supramolecular polymerization of **2** can follow either a kinetic or a thermodynamic pathway depending on the conditions. We also performed the VCD analysis of **3** and **4** by modifying the concentration and temperature. Unlike compound **2**, the sign of the amide I band in **3** and **4** does not change, with a (−/+) pattern observed for the VCD amide I band, regardless of the experimental conditions used (Table 1 and see Figures S9 and S10 in the Supporting Information).

It must be taken into account when rationalizing these phenomena that the structural difference between **2** and **3**/**4** stems from the number of phenyl rings present in the central aromatic moiety. In biphenyls, the steric hindrance exerted by the *ortho* protons of adjacent phenyl rings prevails over the

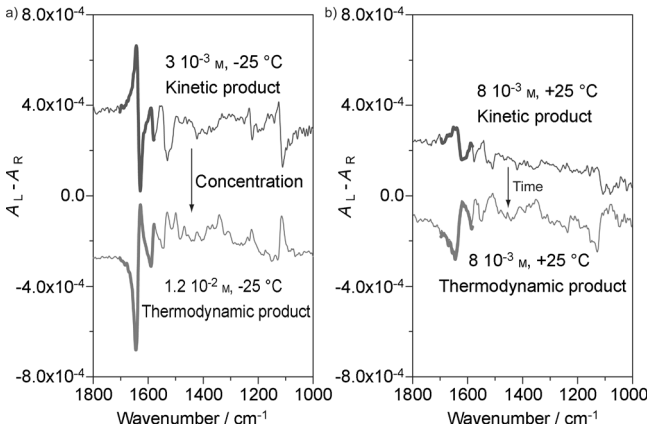

Figure 4. VCD spectra of **2**. a) At high and low concentration (same formation time and temperature). b) As formed ($t_0 = 0$ h) and after 24 h ($t_f = 24$ h) at the same concentration and temperature.

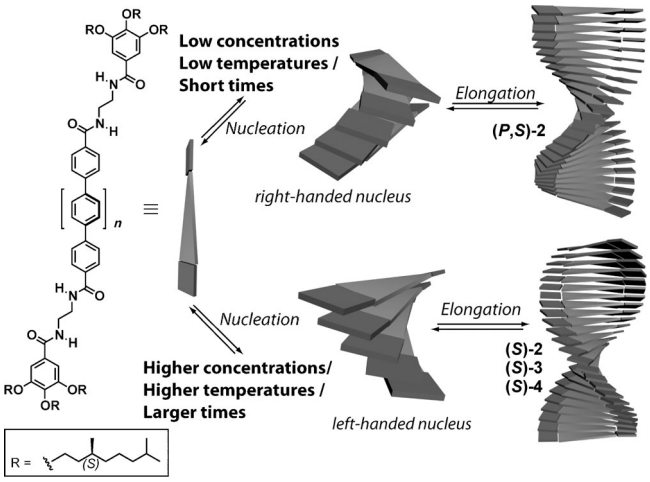

Scheme 1. Schematic illustration of the aggregation pathways of **2**–**4**. At low concentrations, low temperatures, and short times, the helical organization of **2** is dominated by the atropisomerism of the central biphenyl unit, and metastable *P*-type helices are formed. **3** and **4**, and also **2** at higher concentrations, higher temperatures, and longer times, self-assemble into supramolecular structures of the opposite helicity (*M*-type).

coplanarity induced by π conjugation, and this results in a nonplanar conformation of the two inner aromatic units. As a result, the two atropisomers *P* and *M* can exist (see Figure S11 in the Supporting Information).[15] DFT quantum chemical calculations at the B3LYP/6-31G** level were used to predict the VCD spectra of these two atropisomers of **2** (the peripheral *S* stereocenters have been omitted in the models in Figure S11 in the Supporting Information). The calculated amide I bisignated VCD band for the *M* enantiomer is (−/+), which is opposite to that of the *P* enantiomer (+/−). Moreover, no VCD signal for the planar biphenyl conformation was predicted (Figure S11 in the Supporting Information). In the next step of the simulation, we considered the presence of the six peripheral *S* stereocenters, thus generating the corresponding pair of *M*,*S* and *P*,*S* diastereroisomers. The calculated VCD spectrum of the *P*,*S* diastereomer coincides with the experimental VCD spectrum of **2** recorded at low temperature (−25 °C) and low concentration (3×10^{-3} M) (Figure 3c). Additionally, these calculations reveal that the rotational barrier required for the interconversion between the *M*,*S* and *P*,*S* diasteroisomers of **2** is 2.09 kcal mol^{-1} (see Figures S12 and S13 in the Supporting Information).

With all this data together, two different scenarios for the supramolecular polymerization of the reported organogelators are possible. The first concerns the helical organization of **3** and **4**, which is only governed by the peripheral *S* stereocenters, and results in *M*-type helical structures. No exchangeable helicity is observed for **3** and **4** due to the rather planar conformation of the oligophenyl core. The second scenario is exclusive for **2**, which discloses a large dihedral angle between the two innermost phenyl rings, thus allowing two possible atropisomers to enter into play. At low concentration and low temperatures, atropisomerism through the *P*,*S* diastereomer is effective and generates a kinetically controlled situation where *P*-handed nuclei are initially formed (t_0 in Table 1). These further elongate to yield metastable *P*-type supramolecular polymers with a typical (+/−) VCD amide I band (Scheme 1). At higher concentrations (π-π stacking would help to planarize the biphenyl) and higher temperatures (the activation energy or rotational barrier of the biphenyl system is easily overcome) the molecular atropisomerism of **2** is cancelled out, and only the chiral, peripheral *S* stereocenters dictate the helicity of the supramolecular aggregates, which corresponds to the thermodynamically controlled *M*-type helical supramolecular polymerization. Very interestingly, at intermediate concentrations (8×10^{-3} M) and 25 °C, we find a situation where at short times ($t_0 = 0$ h, as formed) the polymerization reaction yields the kinetic *P*-type product, which reverses its helicity after 24 h ($t_f = 24$ h) to a thermodynamically *M*-type final product. This *P*-type→*M*-type helical inversion corroborates the kinetic-versus-thermodynamic modulation of the supramolecular helicity of **2**.

In summary, we have reported on the atropisomerization of helical supramolecular polymers formed by the cooperative self-assembly of oligo-*p*-phenylene-based organogelators **2**–**4**. This helical atropisomerism is driven by the axial chirality of the oligophenyl moieties. In this regard, biphenyl atropisomerism and biphenyl axial chirality are synonymous. The balance between orthogonality and π conjugation of the oligophenyl units induces the molecular atropisomerism, which plays a fundamental part in the expression of the chirality of the supramolecular helices by means of kinetically or thermodynamically controlled polymerization mechanisms. Different techniques (CD, AFM, VCD, ROA, and theoretical calculations) unambiguously demonstrate the left-handed helical organization of polymers of **3** and **4** under all the conditions investigated. Supramolecular polymerization of **2** is highly sensitive to the initial conditions, which drive either a kinetic or thermodynamic pathway to produce helical structures of opposite handedness. Under particular conditions, the kinetic product converts into the thermodynamic one over time. All these data contribute to an increased knowledge and control over the generation of helical supramolecular structures by the synergy of different chiral

elements and could contribute to the development of new optimized strategies to achieve functional supramolecular systems.

Received: October 21, 2013
Published online: December 18, 2013

Keywords: atropisomerism · chirality · helical structures · self-assembly · supramolecular polymers

[1] a) *Mirror-Image Asymmetry: An Introduction to the Origin and Consequences of Chirality* (Ed.: J. P. Riehl), Wiley, Hoboken, **2010**; b) R. Bentley, *Chem. Soc. Rev.* **2005**, *34*, 609 – 624; c) W. L. Noorduin, E. Vlieg, R. M. Kellogg, B. Kaptein, *Angew. Chem.* **2009**, *121*, 9778 – 9784; *Angew. Chem. Int. Ed.* **2009**, *48*, 9600 – 9606.

[2] a) H. C. Kolb, M. S. Vannieuwenhze, K. B. Sharpless, *Chem. Rev.* **1994**, *94*, 2483 – 2547; b) A. Dondoni, A. Massi, *Angew. Chem.* **2008**, *120*, 4716 – 4739; *Angew. Chem. Int. Ed.* **2008**, *47*, 4638 – 4660; c) *Catalytic Methods in Asymmetric Synthesis: Advanced Materials, Techniques, and Applications* (Eds.: M. Gruttadauria, F. Giacalone), Wiley, Hoboken, **2011**.

[3] a) F. Vera, J. Barberá, P. Romero, J. L. Serrano, M. B. Ros, T. Sierra, *Angew. Chem.* **2010**, *122*, 5030 – 5034; *Angew. Chem. Int. Ed.* **2010**, *49*, 4910 – 4914; b) C. Tschierske, *Chem. Soc. Rev.* **2007**, *36*, 1930 – 1970.

[4] a) M. Hasegawa, M. Iyoda, *Chem. Soc. Rev.* **2010**, *39*, 2420 – 2427; b) L. A. P. Kane-Maguire, G. G. Wallace, *Chem. Soc. Rev.* **2010**, *39*, 2545 – 2576; c) P. Iavicoli, H. Xu, L. N. Feldborg, M. Linares, M. Paradinas, S. Stafström, C. Ocal, B. Nieto-Ortega, J. Casado, J. T. López Navarrete, R. Lazzaroni, S. De Feyter, D. B. Amabilino, *J. Am. Chem. Soc.* **2010**, *132*, 9350 – 9362.

[5] a) J. P. Hill, W. Jin, A. Kosaka, T. Fukushima, H. Ichihara, T. Shimomura, K. Ito, T. Hashizume, N. Ishii, T. Aida, *Science* **2004**, *304*, 1481 – 1483; b) M. M. J. Smulders, A. P. H. J. Schenning, E. W. Meijer, *J. Am. Chem. Soc.* **2008**, *130*, 606 – 611; T. E. Kaiser, V. Stepanenko, F. Würthner, *J. Am. Chem. Soc.* **2009**, *131*, 6719 – 6732; c) F. García, P. M. Viruela, E. Matesanz, E. Ortí, L. Sánchez, *Chem. Eur. J.* **2011**, *17*, 7755 – 7759; d) F. García, L. Sánchez, *J. Am. Chem. Soc.* **2012**, *134*, 734 – 742.

[6] F. Aparicio, E. Matesanz, L. Sánchez, *Chem. Commun.* **2012**, *48*, 5757 – 5759.

[7] a) M. Oki, *Top. Stereochem.* **1983**, *14*, 1 – 81; b) J. Clayden, W. J. Moran, P. J. Edwards, S. R. LaPlante, *Angew. Chem.* **2009**, *121*, 6516 – 6520; *Angew. Chem. Int. Ed.* **2009**, *48*, 6398 – 6401; c) B. Paul, G. L. Butterfoss, M. G. Boswell, P. D. Renfrew, F. G. Yeung, N. H. Shah, C. Wolf, R. Bonneau, K. Kirshenbaum, *J. Am. Chem. Soc.* **2011**, *133*, 10910 – 10919.

[8] a) P. Mukhopadhyay, Y. Iwashita, M. Shirakawa, S. Kawano, N. Fujita, S. Shinkai, *Angew. Chem.* **2006**, *118*, 1622 – 1625; *Angew. Chem. Int. Ed.* **2006**, *45*, 1592 – 1595; b) S. Ghosh, X.-Q. Li, V. Stepanenko, F. Würthner, *Chem. Eur. J.* **2008**, *14*, 11343 – 11357; c) A. Dawn, N. Fujita, S. Haraguchi, K. Sada, S. Shinkai, *Chem. Commun.* **2009**, 2100 – 2101.

[9] a) N. Miyaura in *Metal-Catalyzed Cross-Coupling Reactions*, Wiley-VCH, Weinheim, **2008**, pp. 41 – 123; b) N. Miyaura, A. Suzuki, *Chem. Rev.* **1995**, *95*, 2457 – 2483.

[10] a) J. H. van Esch, B. L. Feringa, *Angew. Chem.* **2000**, *112*, 2351 – 2354; *Angew. Chem. Int. Ed.* **2000**, *39*, 2263 – 2266; b) M. George, R. G. Weiss, *Acc. Chem. Res.* **2006**, *39*, 489 – 497; c) M. Sada, N. Takeuchi, M. Fujita, M. Numata, S. Shinkai, *Chem. Soc. Rev.* **2007**, *36*, 415 – 435; d) A. Ajayaghosh, V. K. Praveen, C. Vijayakumar, *Chem. Soc. Rev.* **2008**, *37*, 109 – 122; e) J. W. Steed, *Chem. Commun.* **2011**, *47*, 1379 – 1383.

[11] *Stereochemistry of Organic Compounds* (Eds.: E. L. Eliel, S. H. Wilen, L. N. Mander), Wiley-Interscience, Chichester, UK, **1994**.

[12] The intensity of the bisignated dichroic signal of **4** diminishes but does not disappear upon heating the sample at 90 °C for 1 h at a concentration as low as 5×10^{-7} M, which demonstrates the very strong trend of **4** to aggregate.

[13] G. Yang, Y. Xu in *Electronic and Magnetic Properties of Chiral Molecules and Supramolecular Architectures*, *Vol. 298* (Eds.: R. Naaman, D. N. Beratan, D. Waldeck), Springer, Berlin, **2011**, pp. 189 – 236.

[14] P. A. Korevaar, S. J. George, A. J. Markvoort, M. M. J. Smulders, P. A. J. Hilbers, A. P. H. J. Schenning, T. F. A. De Greef, E. W. Meijer, *Nature* **2012**, *481*, 492 – 497.

[15] a) S. T. Pasco, G. L. Baker, *Synth. Met.* **1997**, *84*, 275 – 276; b) S. Tsuzuki, T. Uchimaru, K. Matsumura, M. Mikami, K. Tanabe, *J. Chem. Phys.* **1999**, *110*, 2858 – 2861; c) L. Lunazzi, A. Mazzanti, M. Minzoni, J. E. Anderson, *Org. Lett.* **2005**, *7*, 1291 – 1294; d) S. Tsuzuki, T. Uchimaru, K. Matsumura, M. Mikami, K. Tanabe, *J. Am. Chem. Soc.* **2008**, *130*, 13867 – 13869.

